

## Electrochemical Behavior of Supercapacitor Electrodes Based on Activated Carbon and Fly Ash

S. Martinović<sup>1</sup>, M. Vlahović<sup>1</sup>, E. Ponomaryova<sup>2</sup>, I.V. Ryzhkov<sup>2</sup>, M. Jovanović<sup>3</sup>, I. Bušatlić<sup>3</sup>, T. Volkov Husović<sup>4</sup>, Z. Stević<sup>5,\*</sup>

<sup>1</sup> University of Belgrade, Institute of Chemistry, Technology and Metallurgy, Belgrade, Serbia

<sup>2</sup> Prydniprovsk State Academy of Civil Engineering and Architecture, Dnipropetrovsk, Ukraine

<sup>3</sup> University of Zenica, Faculty of Metallurgy and Material Science, Zenica, Bosnia and Herzegovina

<sup>4</sup> University of Belgrade, Faculty of Technology and Metallurgy, Belgrade, Serbia

<sup>5</sup> University of Belgrade, Technical Faculty in Bor, Bor, Serbia

\*E-mail: [zstevic@tfbor.bg.ac.rs](mailto:zstevic@tfbor.bg.ac.rs)

Received: 19 January 2017 / Accepted: 8 June 2017 / Published: 12 July 2017

---

The possibility of applying fly ash from power plants as a binder in supercapacitor electrodes based on activated carbon was investigated in this research. Based on the mechanical and electrical properties of the electrodes, the optimal ratio between fly ash and AC was determined. Supercapacitor electrodes were prepared in two ways: by pressing and by laser solidification. The preparation method significantly affected physical properties of the electrodes as well as the electrochemical behavior in supercapacitor setup. The electrodes were electrochemically tested by galvanostatic and potentiostatic methods and cyclic voltammetry. In order to improve the estimation of supercapacitor parameters, mathematical model that perfectly describes the behavior of investigated electrodes in aqueous solution of sodium nitrate was developed. The best results were obtained with laser-solidified electrode in 1M aqueous solution of NaNO<sub>3</sub>. Specific capacitance of 105 F/g, serial resistance of 0.57 Ω and self-discharge resistance of 95 Ω were achieved. Stability at high number of cycles proved to be very good. After 2000 cycles of CV at scan rate of 100 mV/s, specific capacitance fell by only 4.6 %.

---

**Keywords:** supercapacitors; activated carbon; fly ash; laser solidification; NaNO<sub>3</sub>

### 1. INTRODUCTION

Storing energy in electrochemical double-layer capacitors (EDLC) is a result of charge separation at the interface between the electrode as electronic conductor and the electrolyte as ionic conductor of electricity. Capacitance that occurs at that interface is called a double-layer capacitance [1,2].

Due to its high specific surface, activated carbon is one of the standard materials for electrochemical double-layer capacitors. Electrochemical processes that occur at electrochemical double-layer capacitor can be described as follows [3]:

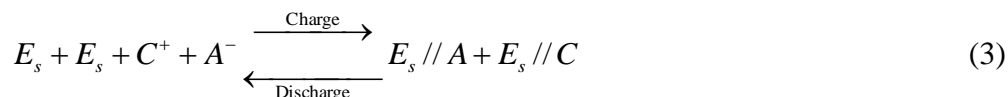
Positive electrode:



Negative electrode:



Overall reaction:



where  $E_s$  is carbon electrode surface area, // is double layer with both sides for charge accumulation,  $C^+$  and  $A^-$  are *cationic and anionic species* present in the electrolyte. Based on the above reactions, it can be concluded that during charging, the electrons are pushed from the positive to the negative electrode by an external source, while at the same time the positive and negative ions separate and move towards the surfaces of electrodes. During discharge through a consumer the electrons move from the negative to the positive electrode, and ions release from the electrodes surfaces and return to the electrolyte. According to the overall reaction, salt ( $C^+A^-$ ) from the electrolyte is consumed during the charging, so that the electrolyte can be considered as active material. Charge density at the electrode-electrolyte interface changes during charging and discharging as well as concentration and conductivity of the electrolyte [4].

Supercapacitors have higher specific power than batteries and for this reason they are combined with batteries in electric devices. Other advantages are related to the longer service life, work in a wider temperature range and fast charge-discharge. Further investigations are directed towards increasing their specific energy [5].

The main factors that dictate choosing carbon for numerous electrochemical applications are its availability, low cost, easy processing, as well as different forms (powder, nano fibers and tubes, foam, fabric, composites) [6] and adjustable porosity [7-11]. Carbon electrodes are well polarisable, chemically stable in various solutions (acidic, basic) and in a wide temperature range. The electrode material has to be electrochemically inert in the potentials operating range, which is limited by the electrolyte decomposition potential [12].

In aqueous solutions supercapacitor voltage cannot exceed 1 V, so it is clear that organic solutions by giving greater energy have significant advantages compared to the water solutions. Unfortunately, organic electrolytes mainly have lower conductivity, which reduces the specific power.

In order to improve the electrical and mechanical properties, supercapacitor electrodes are often made of composite based on carbon and suitable binders (for example poly(vinylidene difluoride) (PVDF) or poly(tetrafluoroethylene) (PTFE)) [13-16]. The possibility of applying ash for this purpose was also investigated [17,18].

Fly ash is formed as waste product in thermal power plants (TPP) fired by coal. The term "fly ash" implies a residue after combustion (for energy purposes) of ground coal, which distinguishes it from all other ashes. In addition, fly ash has specific characteristics significantly different from other ashes and other industrial mineral wastes. The chemical composition of fly ash varies depending on the kind of used fuel and combustion technology while the presence of carbon, whose content can vary from 2 to 10 wt.%, considerably affects the electrical conductivity of the material [19].

The aim of this study was to improve the process of producing supercapacitor electrodes based on active carbon with the addition of fly ash from the power plant as a binder. The composite solidified using laser was compared with the composite obtained by conventional pressing.

## 2. EXPERIMENTAL

### 2.1 Electrode preparation

Preliminary experiments were performed with various ratios of fly ash (FA) and activated carbon (AC) (5, 10, 15 and 20 wt.% FA) and based on mechanical and electrical properties of the electrodes it was determined that optimal composition is 10 wt.% of FA and 90 wt.% of AC. Activated carbon (Aktivkohle, MERCK) was used as basic active material and FA from the Thermal Power Plant "Nikola Tesla A", Obrenovac, Serbia was used as a binder.

Main physical properties of used FA are given in Table 1 and Figure 1.

**Table 1.** Physical properties of FA from TPP "Nikola Tesla A"

Specific surface area (cm <sup>2</sup> /g)	$\gamma$ (g/cm <sup>3</sup> )	$\rho$ ( $\Omega$ m)	LOI (%)
4487.52	0.56	$4.3 \cdot 10^7$	3.75

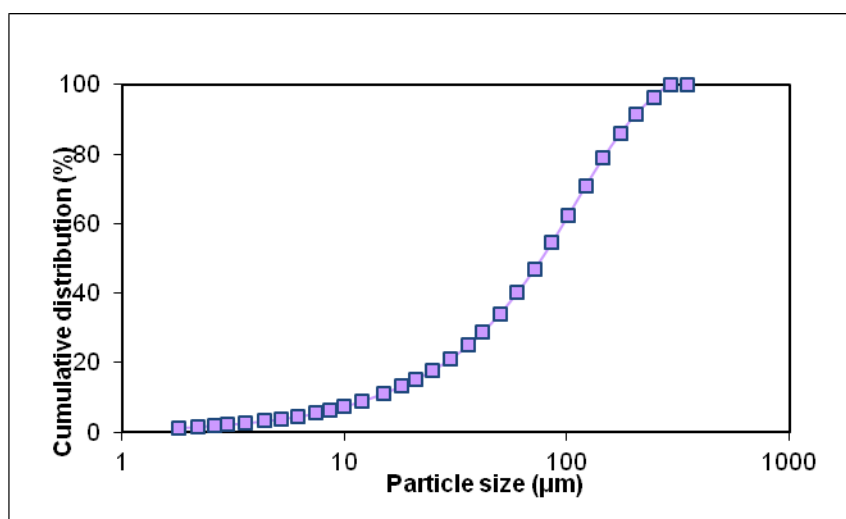


**Figure 1.** Particle size distribution of FA from TPP "Nikola Tesla A".

AC/FA electrodes were prepared using two methods. Method 1 consisted of manual mixing of the components (10 wt.% of FA and 90 wt.% of AC), followed by pressing at different pressures along with gold-plated brass surface. Optimal pressure was  $20 \text{ kN/cm}^2$ , as a compromise between mechanical stability and porosity of the electrode. On the other side of gold-plated substrate copper conductor was soldered and at the end everything except active surface was plastered in the Epofix resin (Epoxyan, Čačak, Serbia). The prepared electrode was marked with  $E_1$ . The construction of the electrode is illustrated in Figure 2, and Figure 3 shows microphotograph of the electrode active surface.

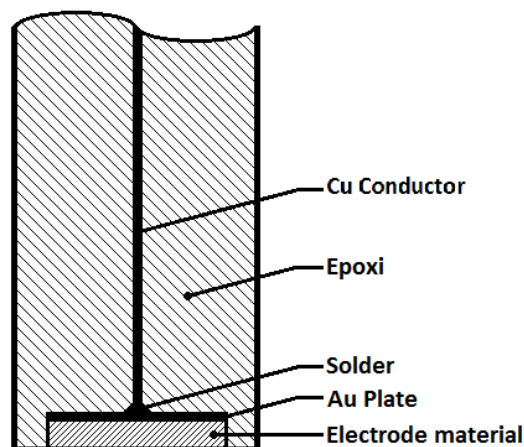


**Figure 2.** Construction of the electrode.

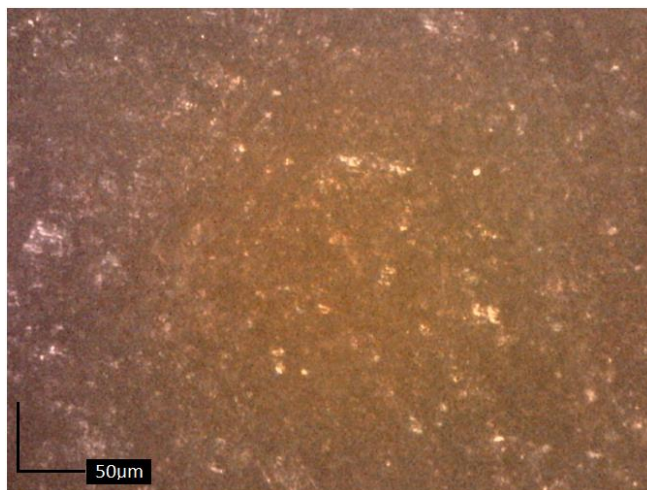


**Figure 3.** Microphotograph of electrode active surface  $E_1$ .

Method 2 is the same as method 1 in all preparation stages, except that laser solidification is applied instead of pressing. Continuous unpolarised semiconductor lasers PGL-F series, CNI (power 2W, wavelength 445 nm) was used for that purpose. The mixture AC/FA was scanned by laser at a rate of 1mm/min; thus compact electrode was obtained, and high porosity remained. Besides reinforcing effect, specific resistance decrease of ash was noticed ( $4.5 \cdot 10^6 \Omega\text{m}$ ). After sealing into the epoxy mass,

the active electrode surface was grinded and polished. It was marked with E<sub>2</sub>. Figure 4 presents microphotograph of the electrode active surface.



**Figure 4.** Microphotograph of electrode active surface E<sub>2</sub>.

## 2.2 Electrochemical testing

Numerous standard testing methods for electrochemical systems can be applied on supercapacitors, with certain modifications [1,20,21]. In this research the method of cyclic voltammetry, galvanostatic method of charging and discharging and potentiostatic method were used.

In order to monitor the process on a single electrode (electrode-electrolyte interface), three-electrode electrochemical cell was used. One of the tested electrodes (E<sub>1</sub> or E<sub>2</sub>) was connected as a working electrode. A saturated calomel electrode (SCE) was used as a reference electrode and a platinum mesh as a counter electrode. Operating electrolyte was 1M aqueous solution of sodium nitrate (NaNO<sub>3</sub>).

The electrochemical cell was connected to a standard galvanostat- potentiostat Interface 1000 from GAMRY Instruments. The system includes software for all necessary electrochemical testing methods. All tests were performed at room temperature.

## 2.3 Mathematical modeling of electrode behavior in NaNO<sub>3</sub> aqueous solution

A simplified analog circuit (Figure 5), which describes well enough behavior of carbon materials in aqueous solutions, was selected starting from the complex model [1,20].

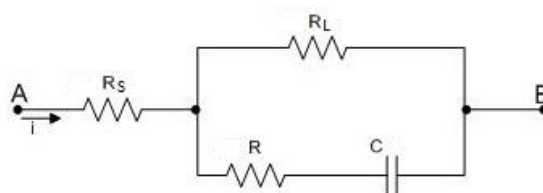


**Figure 5.** Analog electrical circuit.

The resistance  $R_s$  physically corresponds to the resistance of the electrolyte and electrode material with ohm range value. The resistance  $R$  (with tens of ohms range value) is related to the slow adsorption and diffusion processes. Capacitance  $C$  (farad range value) is an integrated capacitance.  $R_L$ , with kilohm range value, is the resistance of self-discharge, therefore it is reciprocally connected with the leakage current.

For adopted analog circuit and applied electrochemical test methods for supercapacitors, in other words for the corresponding excitation, circuit response was analytically determined. Experimentally obtained response diagrams of voltage or current show the validity of the model, while circuit parameters were calculated by entering characteristic read values into a mathematical model.

### 2.3.1 Cyclic voltammetry

Cyclic voltammetry is one of the standard electrochemical methods [1,20]. The analysis of its application for supercapacitors, that is for model presented in Figure 5, is presented in this research.

Excitation overpotential can be analytically presented as:

$$\eta(t) = \frac{E_m}{t_1} t \quad \text{for ascending part (charging phase)} \tag{4}$$

$$\eta(t) = 2E_m - \frac{E_m}{t_1} t \quad \text{for descending part (discharging phase)} \tag{5}$$

With real assumption that  $R_s+R \ll R_L$ , analysis of circuits leads to simplified expressions for the current in the time domain and in a quasi-stationary regime (after several cycles):

$$i(t) = \frac{E_m}{t_1} C \left( 1 - 2e^{-\frac{t}{\tau}} \right) \quad \text{charging phase} \tag{6}$$

$$i(t) = \frac{E_m}{t_1} C \left( 2e^{-\frac{t}{\tau}} - 1 \right) \quad \text{discharging phase} \tag{7}$$

$$\frac{di}{dt}_{t \rightarrow 0} = \frac{2E_m}{(R_s+R)t_1} \tag{8}$$

$$\tau = (R_s+R)C \quad \text{time constant of charging/discharging} \tag{9}$$

Time is measured from the beginning of each phase. Besides capacitance, equivalent serial resistance  $R_s + R$  is one of the most important parameters of supercapacitors. Usually it is represented by the abbreviation ESR.

Plateau current, that is maximum current will be:

$$I_{\max} = -I_{\min} = \frac{E_m}{t_1} C \tag{10}$$

Integral capacitance C can be directly calculated by entering  $I_{\max}$  read from the experimentally obtained diagram into the Equation (10). However, in some cases, current plateau is not pronounced, so that calculating C from the area A marked by the curve  $i-\eta$  is more reliable:

$$C = \frac{At_1}{2E_m^2} \tag{11}$$

Time constant  $\tau$  is obtained from the intercept, and then the total series resistance (ESR) is calculated from the Equation 9.

Self-discharge resistance value  $R_L$  of good supercapacitors is high, but does not affect the shape of the curve CV. Therefore, it cannot be determined by CV method. In the case of pronounced self-discharge, a slightly rising straight line, whose slope is reciprocally linked with  $R_L$ , will appear instead of the current plateau.

### 2.3.2 Galvanostatic charging and discharging

For the assumed analog electrical circuit (Figure 5), the Equation for overpotential  $\eta$  during charging by constant current  $I$  is derived as follows:

$$\eta(t) = (R_s + R)I + R_L I \left( 1 - e^{-\frac{t}{\tau}} \right) \tag{12}$$

where:

$$\tau = R_L C \text{ (time constant)} \tag{13}$$

Typical shape of galvanostatic curve with characteristic data that can be used to calculate all parameters of the equivalent electrical circuit, is shown in Figure 8.

If complete electrochemical curve is recorded (for the pulses duration greater than  $4\tau$  with the aim to achieve stationary level of  $\eta_m$ , which is quite a long time), the procedure for obtaining the circuit parameters would be as follows:

1.  $\eta_m = R_L I$  (14)

is read from the diagram, where:

$$R_L = \frac{\eta_m}{I} \tag{15}$$

2.  $\eta_0 = (R_s + R) I = ESR I$

is read, so

$$ESR = \frac{\eta_0}{I} \tag{16}$$

3. From the read time constant  $\tau$  and (13), capacitance is calculated:

$$C = \frac{\tau}{R_L} \tag{17}$$

Since the time constant  $\tau$  is very large in this case, the current direction  $I$  often changes after the charging to some extent (less than 1 V for the aqueous solutions) and therefore supercapacitor would discharged by exponential law as well.

Overpotential drop 2 I ESR occurs at the time of changing the current direction, from where ESR can be determined more precisely. In this case, the capacitance  $C$  is calculated from the slope of initial (linear) part of charging curve:

$$\frac{d\eta}{dt} = \frac{I}{C} \tag{18}$$

### 2.3.3 Potentiostatic method

If the excitation of electric circuit from the Figure 5 is long overpotential pulse, response of the system (current in this case) will be:

$$i(t) = (I_0 - I_L)e^{-\frac{t}{\tau}} + I_L \tag{19}$$

where:

$$I_0 = \frac{E}{R_s + R} \text{ - initial charging current} \tag{20}$$

$$I_L = \frac{E}{R_s + R_L} \text{ - final charging current (leakage current)} \tag{21}$$

$$\tau = (R_s + R)C \text{ - time constant} \tag{22}$$

Based on the experimentally obtained current diagram, after the reading of  $I_0$ ,  $I_L$  and  $\tau$ , parameters of the circuit can be determined:

$$R_L = \frac{E}{I_L} \tag{22}$$

$$ESR = \frac{E}{I_0} \tag{23}$$

$$C = \frac{\tau}{ESR} \tag{24}$$

This method has the great advantage compared to others. Resistance  $R_L$  can be determined most reliable from the clearly perceptible horizontal part of the curve. Also,  $R_L$  can be accurately determined by the method of self-discharge. However, the time constant  $\tau = R_L C$  is much greater in that case, so experiment lasts long time.

### 2.3.4 Energy density, power density and leakage time constant

Some important characteristics of supercapacitors can be determined using the obtained parameters of equivalent electrical circuit (ESR,  $R_L$  and  $C$ ). These are the energy density ( $W_s$ ), the power density ( $P_s$ ) and the leakage time constant ( $\tau$ ):

$$W_s = \frac{1}{2} C E_m^2 \tag{25}$$

$$P_s = \frac{E_m^2}{ESR} \tag{26}$$

$$\tau_L = CR_L \tag{27}$$

### 3. RESULTS AND DISCUSSION

A series of experiments were done while the representative results obtained by different methods of electrochemical tests are presented here.

#### 3.1 Cyclic voltammetry

Cyclic voltammograms for electrodes E<sub>1</sub> and E<sub>2</sub> in 1M aqueous solution of sodium nitrate (NaNO<sub>3</sub>) at the overpotential changes speed of 2 mV/s are shown in Figure 6. For comparison purpose, results from the Ref [13] are shown in Figure 10 as well.

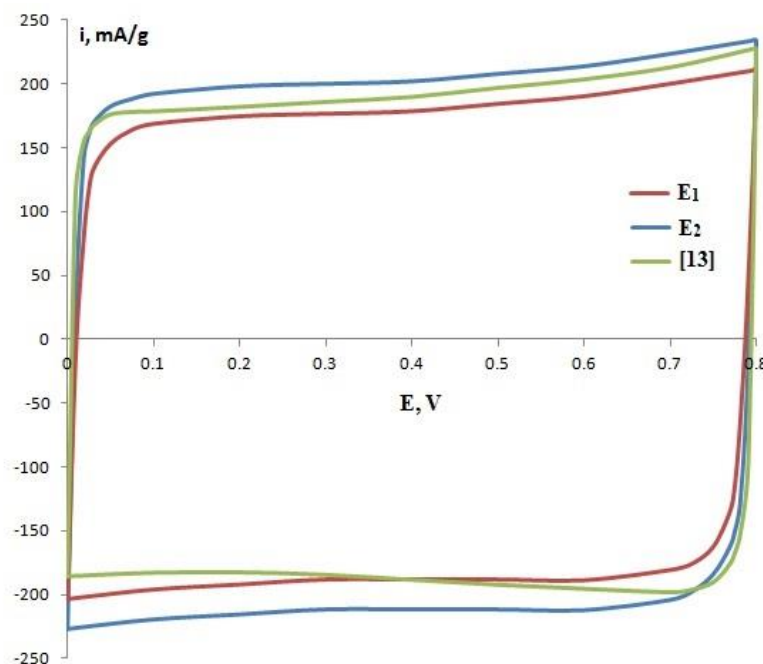


**Figure 6.** Cyclic voltammograms of tested electrodes (E<sub>1</sub> and E<sub>2</sub>) and AC-PTFE composite.

From the diagram shape, it is obvious that the best electrode is E<sub>2</sub> (composite AC/FA solidified by laser). The largest area of loop indicates greater capacitance, while the existence of power plateau means high self-discharge resistance R<sub>L</sub> (not case in the AC/PTFE sample [13]). Electrode E<sub>1</sub> (pressed composite AC/FA) is inferior to the samples E<sub>2</sub> and [13] in terms of capacitance and ESR, but (similar to E<sub>2</sub>) is excellent in terms of self-discharge.

Quantitatively expressed results obtained by the Equations (6-11) are given in Table 2.

**Table 2.** Parameters of supercapacitors determined by the method of cyclic voltammetry

Parameter	Sample	E <sub>1</sub>	E <sub>2</sub>	AC/PTFE [13]
ESR, Ω		0.798	0.569	0.46
C, F/g		92.1	104.9	99.2

It is obvious that the laser-solidified electrode E<sub>2</sub> showed the best results. Stability testing of E<sub>2</sub> exhibited that capacitance dropped for 4.61 % after 2000 CV cycles at a scan rate of 100 mV/s.

In order to verify the model and obtained results, galvanostatic tests were carried out. Experimental diagrams for electrodes E<sub>1</sub> and E<sub>2</sub> in 1M aqueous solution of sodium nitrate (NaNO<sub>3</sub>) at the amperage of 100 mA/g and pulse duration of 800 s are shown in Figure 7.

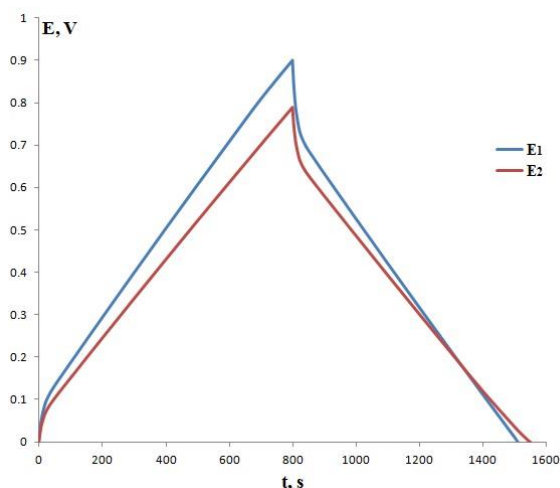


**Figure 7.** Galvanostatic diagrams for electrodes E<sub>1</sub> and E<sub>2</sub>.

Parameters of supercapacitor ESR and C were calculated by reading the characteristic values from the experimental diagrams and applying the Equations 16 and 18, Table 3.

**Table 3.** Parameters of supercapacitors determined by the galvanostatic method

Parameter	Sample	E <sub>1</sub>	E <sub>2</sub>
ESR, Ω		0.795	0.567
C, F/g		92.2	105.1

Due to the accuracy of reading, more accurate ESR value is obtained by this method, while the value of C is more accurate using CV method. However, the results are in very good agreement.

3.3 Potentiostatic method

With the aim of more accurate determination of important supercapacitor parameters, self-discharge resistance  $R_L$ , potentiostatic tests were done.

Time diagram of responsive current for electrodes  $E_1$  and  $E_2$  in 1 M aqueous solution of sodium nitrate ( $\text{NaNO}_3$ ), at potentiostatic pulse with intensity of 100 mV and duration of 500 s is shown in Figure 8.

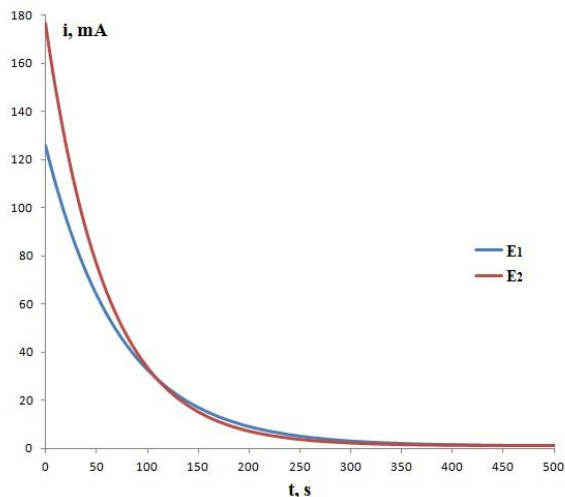


Figure 8. Potentiostatic diagrams for electrodes  $E_1$  and  $E_2$ .

The intercepts, height of the horizontal (final) part of the curve and slope of the initial part of the curve are clearly visible in the diagram, so all important parameters of supercapacitor can be obtained by applying the Equations 22-24, Table 4.

Table 4. Parameters of supercapacitors determined by the potentiostatic method

Parameter	Sample	$E_1$	$E_2$
ESR, $\Omega$		0.794	0.566
$R_L$ , $\Omega$		96.8	95.1
C, F/g		91.8	104.8

Using this method and relatively short experiment, quite accurate values of self-discharge resistance  $R_L$  can be obtained, while other methods are used only for qualitative analysis. Thereby, the value of ESR is determined very precisely by this method, while the CV method is inviolable for determining the capacitance C.

Comparing the results from the Table (2-4), it is obvious that ESR and C are in very good agreement so the proposed model corresponds to the observed system. Also, obtained values are comparable with results of the other studies engaged with AC in aqueous solutions [13-15].

### 3.4 Energy density, power density and leakage time constant

The other important parameters,  $W_s$ ,  $P_s$  and  $\tau_L$ , are calculated using the basic parameters of super capacitors (ESR,  $R_L$  and C) and based on the Equations 25-27 and shown in Table 5.

**Table 5.** Energy density, power density and leakage time constant

Parameter	Sample	E <sub>1</sub>	E <sub>2</sub>
$W_s$ , Wh/kg		8.196	9.324
$P_s$ , W/kg		806	1130
$\tau_L$ , s		8915	9976

Obtained values are comparable with results of the other studies engaged with AC in aqueous solutions [13,14]. Thereby, significant advantages show the laser-solidified electrode E<sub>2</sub>.

## 4. CONCLUSION

Testing of AC/FA composite in aqueous solution of sodium nitrate was carried out in order to optimize electrochemical system for obtaining the best possible properties (as much as possible specific capacitance, the lowest series and the highest parallel resistances). Simplified equivalent electrical circuit that well describes the behavior of observed electrochemical system was selected. Mathematical model that enabled determination of the system parameters was developed based on the electrical circuit and using the experimental results at different excitations. Optimization of the electrode synthesis was also realized. Besides the conventional pressing, the possibility of solidification by laser was also tested and it showed good results. Optimized electrodes (pressed and solidified by laser) were examined by selected electrochemical methods (cyclic voltammetry, galvanostatic and potentiostatic methods). Obtained results showed validity of the proposed model and the electrode material, particularly AC/FA composite solidified by laser.

## ACKNOWLEDGMENTS

This research has been financed by Ministry of Education, Science and Technological Development of the Republic of Serbia as part of the projects TR 33007, III 45012 and ON 172060.

## References

1. B.E.Conway, Electrochemical supercapacitors, Kluwer Academic/Plenum Publishers, (1999) New York, USA.

2. R. Kotz, M. Carlen, *Electrochim Acta*, 45 (2000) 2483.
3. J.P. Zheng, J. Huang and T.R. Jow, *J Electrochem Soc*, 144 (1997) 2026.
4. M. Rajčić-Vujasinović, Z. Stanković, Z. Stević, *Elektrokhimiya*, 35 (1999) 347.
5. C. Liu, Z. Yu, D. Neff, A. Zhamu and B.Z. Jang, *Nano Lett*, 10 (2010) 4863.
6. Z. Q. Gong, A. N. A. Sujari and S. Ab Ghani, *Electrochim Acta*, 65 (2012), 257.
7. K. Pokpas, S. Zbeda, N. Jahed, N. Mohamed, P. G. Baker, and E. I. Iwuoha, *Int J Electrochem Sci*, vol. 9 (2014) 736.
8. B.K. Kim, S. Sy, A. Yu and J. Zhang, *Electrochemical Supercapacitors for Energy Storage and Conversion*, John Wiley & Sons, Ltd., (2015).
9. E. Frackowiak and F. Béguin, *Carbon*, 39 (2001) 937.
10. W. Xing, S.Z. Qiao, R.G. Ding, F. Li, G.Q. Lu, Z.F. Yan and H.M. Cheng, *Carbon*, 44 (2006) 216.
11. Z. Wen, D. Lu, S. Li, J. Sun and S. Ji, *Int J Electrochem Sci*, 9 (2014) 1.
12. A. González, E. Goikolea, J.A. Barrena and R. Mysyk, *Renew Sust Energ Rev*, 58 (2016) 1189.
13. Q. Abbas, D. Pajak, E. Frackowiak and F. Béguin, *Electrochim Acta*, 140 (2014) 132.
14. Z. Zhu, S. Tang, J. Yuan, X. Qin, Y. Deng, R. Qu and G.M. Haarberg, *Int J Electrochem Sci*, 11 (2016) 8270.
15. B. Gao, Y. Li, Y. Tian and L. Gai, *Int. J. Electrochem. Sci.*, 12 (2017) 116
16. A. Ajina and D. Isa, *J Sci & Technol*, 18 (2010) 351.
17. L. Weinstein and R. Dash, *Materials Today*, 16 (2013) 356.
18. Y.M. Chen and H.Y. Zhang, *Adv Mater Res*, 150-151 (2011) 1560.
19. D. Jozić, Studija utjecaja letećeg pepela iz termoelektrane na fizikalno-kemijska svojstva i ponašanje cementnog kompozita, doktorska disertacija, Sveučiliste u Splitu, Kemijsko-tehnološki fakultet, Split (2007).
20. Z. Stevic, M. Rajcic-Vujasinovic and I. Radovanovic, *Int J Electrochem Sci*, 9 (2014) 7110.
21. Z. Stevic, M. Rajcic-Vujasinovic, I. Radovanovic, V. Nikolic, *Int J Electrochem Sci*, 10 (2015) 6020.